# Autonomous Hanging Tether Management and Experimentation for a UAV-USV Team: Sea Trials

## Kurt Talke

Unmanned Systems Advanced Development Branch Naval Information Warfare Center, Pacific San Diego, USA kurt.a.talke.civ@us.navy.mil Frederick Birchmore
Autonomous ISR Branch
Naval Information Warfare Center, Pacific
San Diego, USA
frederick.c.birchmore.civ@us.navy.mil

Abstract—This paper considers the mission of a UAV-USV team where a small unmanned surface vehicle (USV) is tethered to an unmanned air vehicle (UAV). In contrast to a majority of existing tethered UAV work, which assumes a taut tether, this paper addresses the challenge of managing a slack, hanging tether in a dynamic ocean environment up to sea state 4 on the Douglas scale. Our previous work developed and experimentally validated a prototype smart-reel system for a UAV-USV team in a lab-based environment. That system used a reference model for tether control based on static catenary cable theory that equally weighted an increase in tether tension with the risk of fouling the tether with the USV or water. In conjunction, a Kalman filter was developed - fusing slow (4 Hertz) differential GPS (dGPS) relative position measurements with fast (100 Hertz) inertial measurements. The output of the Kalman filter, a 100 Hertz estimate of relative position, was fed into the tether length reference model and a gain-scheduled proportionalderivative (PD) controller drove the smart-reel system to the desired tether length. This paper presents an extension of that work to controlled on-water dynamic wave experimentation and randomized excitation through sea trials.

A surrogate UAV was used in wave-pool experimentation to tune the Kalman filter for on-water use. Using this tuned filter, nine separate UAV flights successfully validated the slack tether management approach in varying head-on wave heights up to 1.0 m as well as two trials of random period irregular wave heights of 0.6 m. The trials were performed using alternating feedback methods for relative position: first using ground-truth motion capture feedback and then using Kalman filter feedback with derated ground-truth to replicate the dGPS sensor at 4 Hertz. The experiments showed robustness to the heave and pitch motions of the USV, effectively decoupling its motion from that of the UAV. The resulting effect is an increased payload capacity and altitude limits for the UAV. In addition to successfully demonstrating the ability to manage a slack tether, reflective markers were added to the tether to generate a unique UAV-tether-USV dynamic motion dataset. This data will be used to validate tether dynamic simulation models in ongoing work.

Following indoor wave-pool testing, the dGPS system was upgraded to a newer model which outputs an 8 Hertz measurement. Significant effort was put into the setup of the radios on each end of the tether (TCP/IP with 921600 Baud) to limit latency to ensure that no dGPS packets were dropped. Our initial sea-based experimental testing revealed that the catenary

Funding for this work is provided by the Department of Defense SMART Scholarship for Service program and Naval Information Warfare Center Pacific under the Naval Innovative Science and Engineering program. Special thanks to Naval Surface Warfare Center Carderock for facilitating access and use of the Maneuvering and Seakeeping Basin.

reference model for tether control needed to be modified to be gain-scheduled for relative position ratios  $(\Delta r/\Delta z)$  up to 10. Lastly, significant effort was put into the software system to ensure that the timing of the digital control system was as deterministic as possible. By ensuring that the Kalman filter, controller, and output command to the motor all occur at their target frequencies, any buildup of errors and delays was minimized - resulting in improved performance. For sea trials, a new waterproof electronics enclosure was developed using industrial electronic components (as we learned during wave-pool testing that Murphy's Law tends to hold true: anything that can break will break), and the smart-reel system was installed on the bimini of a small 6.5 m Boston Whaler. Three separate 30 minute flights were performed at anchor just outside San Diego Bay. The tether management system operated effectively and the experiment was a success.

The development and validation of an autonomous hanging tether management system for a UAV-USV team operating in a dynamic ocean environment up to sea state 4 is a significant technical achievement with far-reaching implications. The system's ability to manage a slack, hanging tether has been validated through both wave-pool testing and on-water sea trials, demonstrating robustness to heave and pitch motions of the USV, increasing the UAV's payload capacity and altitude limits. Additionally, the generation of a unique UAV-tether-USV dynamic motion dataset provides a valuable resource for validating tether dynamic simulation models. Beyond military applications, this system has potential benefits for various industries including fishing, environmental conservation efforts, and other oceanographic research. This work represents a significant step forward in the development of autonomous, long-endurance, tethered UAVs.

Index Terms—Tethered Aerial Systems; UAV; USV; Controls; Kalman Filtering;

#### I. Introduction

Tethered multi-rotor unmanned air vehicles (UAVs) have become widely prevalent in the surveillance, communications, and first-responder communities and readily available in recent years due to a number of different commercially available products. The tether, acting as a power and data umbilical, allows a UAV to overcome its most significant limitation: short-duration missions often limited to less than 30 minutes [1]. By not carrying a heavy power source, a UAV's payload capacity increases significantly and its endurance becomes essentially infinite [2]–[4]. Unfortunately, a tether conversely limits the mobility of the UAV and introduces the challenge

of tether management. Tethered flight is also accompanied by some payload limitations as it introduces additional downward forces on the UAV due to tether weight and tension. These forces must be overcome by increasing UAV thrust – potentially reducing the UAV payload capacity, available power budget, and limiting flight altitude.

The majority of tethered-UAV systems employ a taut tether management approach to avoid tether oscillations [5], improve flight stability [6]–[10], or enhance landing capability [11]–[13]. Such systems neglect the reduced payload capacity and increased UAV thrust requirement by employing either no tether management while the UAV maintains tension with linear [8] and nonlinear flight controllers [14] or by employing a tension-monitoring winch mechanism that continuously reels in any slack tether length [15]. These tethered systems consider only a scenario where the base station is stationary – not undergoing dynamic motion. Other work has considered tethered-UAVs with moving platforms but under taut conditions and with no experimental validation [16]. One such unique application uses a taut tethered-UAV to control the surge dynamics of a floating buoy in simulation [17]–[19].

Other systems have considered non-taut-tethered flight using a reactive tether management approach [20]. Adding a tether to a UAV provides the opportunity to measure additional variables (such as the rotational position and velocity of the reel, tether tension, and tether departure angle) which can be used to perform non-GPS-based UAV position estimation. For instance, the tether arrival angle at the UAV can be measured [21] and/or the tension at the UAV estimated [22] and incorporated into the state estimation algorithm. Other prior related work have used a non-taut catenary cable model for position estimation of the UAV [23]–[25].

In all the existing taut-tethered-UAV work described, no experimental validation has been performed from a highly dynamic moving base station - such as a tethered-UAV mounted on the back of a moving ground vehicle travelling over a rolling road or a small surface vehicle in an ocean environment. In such scenarios, a taut tether management approach may eventually cause the UAV's flight controls to saturate which would force an emergency landing. Additionally, a taut tether management approach would be problematic for any sensor payload that requires the UAV to be stationary since the motion of the UAV is coupled with the base station. Our previous work approached the challenge of a tethered-UAV system flown from a small ocean-going surface vehicle by relaxing the taut tether requirement [26]. We developed a tether management reference model, controller, and estimator to automatically reel in/out the tether to a desired heave-robustness tether length while preventing the tether from fouling with the USV. Compared to taut-tether UAV operation, the use of a hanging tether was shown to minimize the downforce that the tether applies to the UAV – ultimately decreasing power consumption by the UAV-USV team while maintaining the required margins of safety on the thrust of the UAV. The varying sag of the tether inherently compensates for the fastacting dynamics of an ocean environment. Flying on a non-

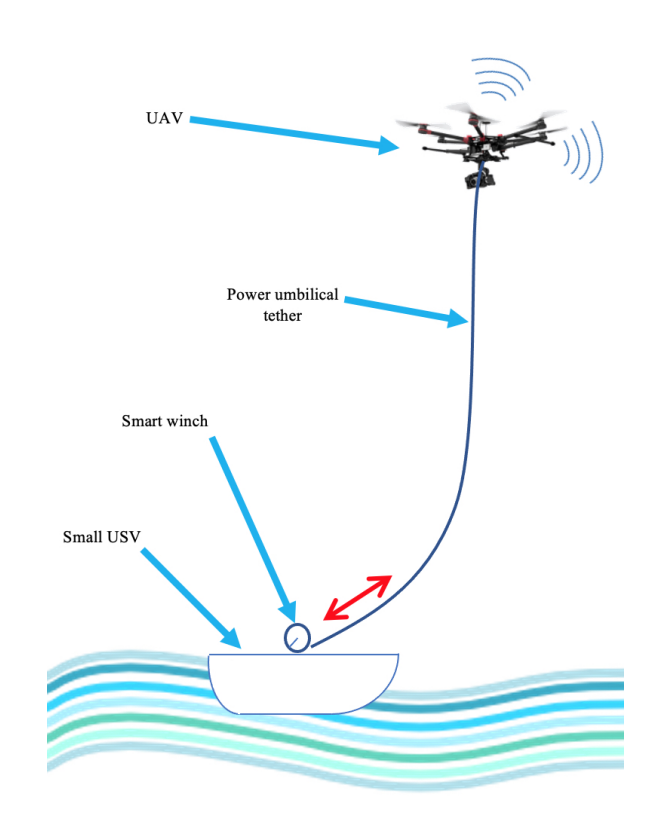


Fig. 1. Schematic of a tethered-UAV-USV team in an ocean environment with waves up to sea state 4. The smart-reel system controls the tether length to account for the dynamic motion of the small USV – leaving the tether in a semi-slack, quasi-static state at all times.

taut, or hanging tether, was shown to effectively decouple the motion of the UAV and the USV in lab-based experimentation.

This paper presents an extension of our prior work to controlled on-water dynamic wave-pool experimentation, an update to the reference tether length model through gain scheduling, hardware and software improvements, and random dynamic excitation validation through ocean sea trials. The remainder of this paper is organized as follows: Section II reviews the pertinent baseline from our prior work. Section III details the indoor wave-pool experimental testing and results. Section IV details the outdoor sea trials and results. Section V provides a summary of the main conclusions.

# II. RECAP OF PRIOR WORK

The UAV, flying at up to 50 m altitude, must maintain position, orientation, and altitude for communication during intelligence, surveillance, and reconnaissance (ISR) missions as shown in Figure 1. The UAV is tethered to a small unmanned surface vehicle (USV) with a length of 3 to 7 meters – which is subject to a dynamic ocean environment. We developed and experimentally validated a prototype smartreel system and controller for a UAV-USV team in a labbased environment using a wave-and-boat-motion-replication mechanism [27]. This system used a reference model for tether control based on static catenary cable theory which equally

weighted an increase in tether tension with the risk of fouling the tether with the USV or with water [28].

## A. Catenary Tether Reference Model

The relative position ratio,  $\Delta r/\Delta z$ , or ratio of radial distance to altitude, was used to nondimensionalize the reference model. For the relative position ratio,  $\Delta r/\Delta z \leq 1.1$ , a third order polynomial model is used:

$$L_{ref} = \Delta z \left( c_1 + c_2 \frac{\Delta r}{\Delta z} + c_3 \frac{\Delta r^2}{\Delta z^2} + c_4 \frac{\Delta r^3}{\Delta z^3} \right)$$
 (1)

with coefficients  $c_1=0.9964$ ,  $c_2=0.1514$ ,  $c_3=0.4674$ , and  $c_4=-0.1280$ , and for  $\Delta r/\Delta z \geq 1.3$ , a second order polynomial model is used:

$$L_{ref} = \Delta z \left( d_1 + d_2 \frac{\Delta r}{\Delta z} + d_3 \frac{\Delta r^2}{\Delta z^2} \right)$$
 (2)

with coefficients  $d_1 = 0.9748$ ,  $d_2 = 0.2615$ , and  $d_3 = 0.2370$ . In the region between,  $1.1 < \Delta r/\Delta z < 1.3$ , a linear combination of the second and third order models is used in order to smooth the transition. By measuring the radial distance between the winch, the UAV, and the UAV altitude, a tether length that is robust to heave can be determined.

## B. Sensing and Estimation Filter

A linear, double-integrator Kalman filter model was developed in conjunction with the reference model, which is restricted to the altitude degree-of-freedom (DOF) and fuses slow (4 Hertz) differential GPS (dGPS) relative position measurements with fast (100 Hertz) inertial measurements:

$$\Delta z_{k+1} = \Delta z_k + \Delta t \Delta \dot{z}_k + \omega_{z,k} \qquad \omega_z = \mathcal{N}(0, \sigma_z^2)$$

$$\Delta \dot{z}_{k+1} = \Delta \dot{z}_k + \Delta t \Delta \ddot{z}_k + \omega_{\dot{z},k} \qquad \omega_{\dot{z}} = \mathcal{N}(0, \sigma_z^2)$$

$$\Delta \ddot{z}_{k+1} = \Delta \ddot{z}_k + \omega_{\ddot{z},k} \qquad \omega_{\ddot{z}} = \mathcal{N}(0, \sigma_z^2) \qquad (3)$$

$$\mu_{1,k+1} = \mu_k + \omega_{\mu_1,k} \qquad \omega_{\mu_1} = \mathcal{N}(0, \sigma_{\mu_1}^2)$$

$$\mu_{2,k+1} = \mu_k + \omega_{\mu_2,k} \qquad \omega_{\mu_2} = \mathcal{N}(0, \sigma_{\mu_2}^2)$$

where  $\Delta z$ ,  $\Delta \dot{z}$ ,  $\Delta \ddot{z}$  are the relative position, velocity, and acceleration, respectively,  $\mu_1$  and  $\mu_2$  are the estimated accelerometer biases, and  $\Delta t$  is the timestep of the filter running at 100 Hertz. All states are assumed to have zero mean and normally-distributed system noise. The measurement model is defined as:

$$\Delta z_{GPS,k} = \Delta z_k + v_{z,k} \qquad v_z = \mathcal{N}(0, \sigma_{dGPS}^2)$$

$$\Delta \ddot{z}_{Acc_1,k} = \Delta \ddot{z}_k + \mu_{1,k} + v_{\ddot{z}_1,k} \quad v_{\ddot{z}_1} = \mathcal{N}(0, \sigma_{Acc_1}^2) \quad (4)$$

$$\Delta \ddot{z}_{Acc_2,k} = \Delta \ddot{z}_k + \mu_{2,k} + v_{\ddot{z}_2,k} \quad v_{\ddot{z}_2} = \mathcal{N}(0, \sigma_{Acc_2}^2)$$

where  $\Delta z_{dGPS}$  is the dGPS measurement and  $\Delta \ddot{z}_{Acc_1}$  and  $\Delta \ddot{z}_{Acc_2}$  are the vertical accelerations from two inertial measurement units (IMUs). All measurements are assumed to have zero mean, normally-distributed measurement noise. The estimation filter facilitates operations beyond the lab environment – allowing for experimental validation outdoors.

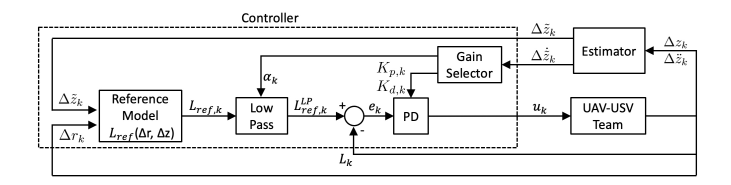


Fig. 2. Tether management controller: The polynomial model uses the relative position of the UAV and USV to determine a reference length. The spool encoder measurement is compared to the reference length to generate an error signal. A proportional-derivative (PD) controller on the spool motor commands the spool to pay out or reel in tether. The low-pass filter coefficient and the controller gains are gain-scheduled based on the estimated relative velocity.

## C. Controller

The output of the Kalman filter, a 100 Hertz estimate of relative position, was fed into the tether length reference model and a gain-scheduled proportional-derivative (PD) controller drove the smart-reel system to the desired tether length as seen in Figure 2. A gain-scheduled low-pass filter was used on the reference tether length,  $L_{ref,k}^{LP}$ , in order to to smooth out any discontinuities in the relative altitude estimate at slow speeds.

## D. Smart-Reel System

Our previous work developed a smart-reel prototype with a passive-tether departure angle measurement approach. Although we demonstrated that this approach had promise, our feedback controller is not reliant on this measurement. A redesigned and simplified smart-reel design is shown in Figure 3. The key improvements over our prior design are a more

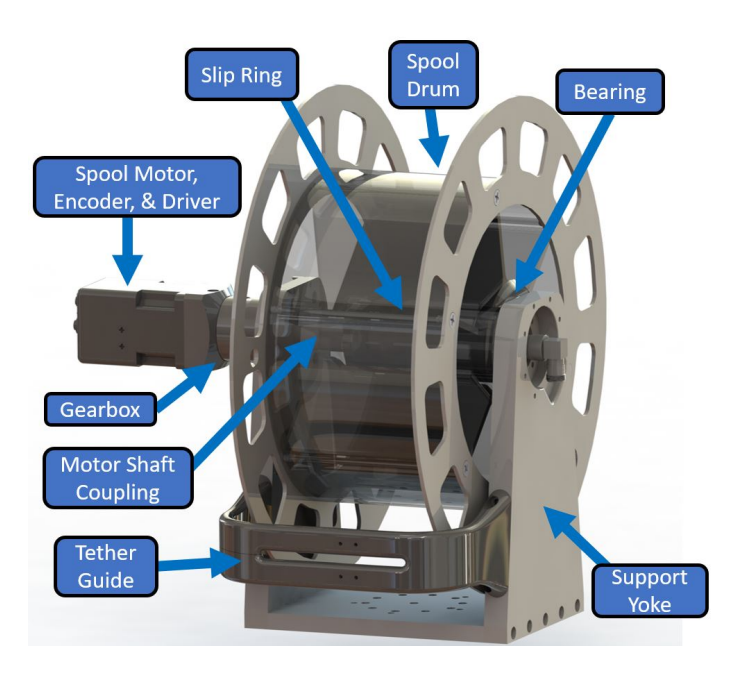


Fig. 3. Updated and redesigned smart-reel prototype capable of spooling 100 m of 4.5 mm diameter tether with a 50 mm minimum bend radius. The integrated sensors can measure the tether length and motor torque

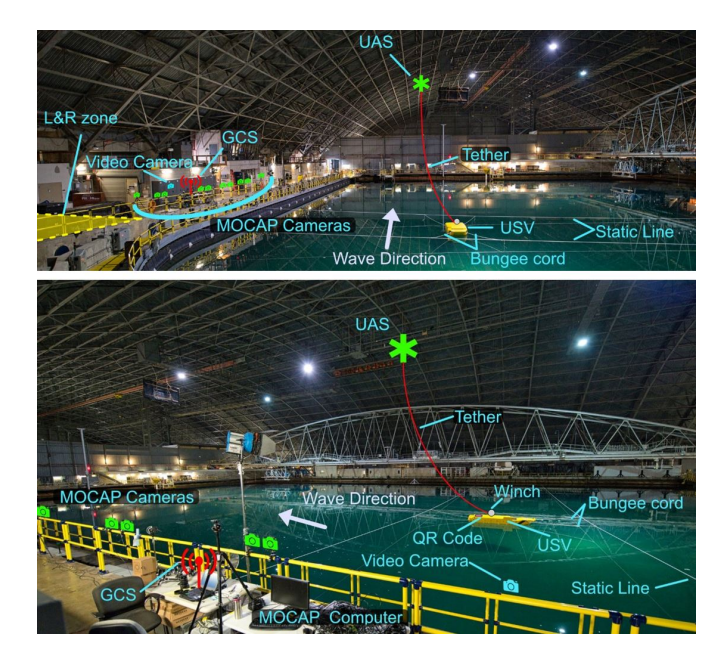


Fig. 4. MASK test setup front and side views – showing the USV, wave direction, static guide lines, motion capture system setup, and operating position of the UAV.

rigid structure, the removal of the passive tether departure measurement capability, in favor of a fixed tether exit channel.

## III. MASK INDOOR WAVE-POOL TESTING

The updated smart-reel system underwent experimental validation at the Maritime and Seakeeping (MASK) Basin at Naval Surface Warfare Center (NSWC) Carderock. The facility has a 110 m by 73 m indoor wave-pool with the capability of generating waves of up to 1.5 m at a 4-second period, and a 30 m high bay over the test section for flying a UAV. The wave maker is equipped with 216 individually-controlled paddles along the short and long edges of the basin, while the opposing edges feature concrete beaches that absorb at least 92% of the wave energy.

# A. MASK Experimental Test Setup

The smart-reel system was mounted to a small 4 m surface vehicle which was held in-position by two sets of guide lines. After launching the UAV from shore, the tether management system was activated, and wavemaker generated head-on waves up to 1.5 m. A motion capture system was setup on shore and streamed the position data of markers on the vessel, UAV, and tether at a frequency of 100 Hertz with a measurement error of less than 0.2 mm. Figure 4 shows the experimental test setup.

To initially validate the smart-reel system, a surrogate UAV was mounted to a catwalk 20 m above the surface of the water. Eight separate experiments with waves ranging from flat water up to 1.0 m were conducted using feedback from the motion capture system. The data from those experiments was then used as a ground-truth cost metric for tuning the Kalman filter gains using a twiddle algorithm as described in our prior work

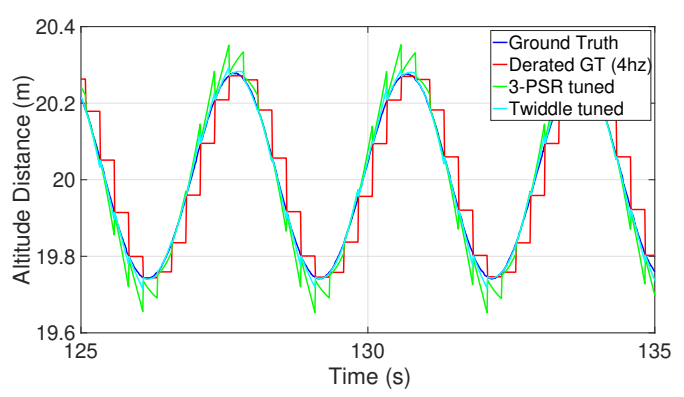


Fig. 5. Typical twiddle tuning results for a consistent 0.6 m, 3 second period wave, showing the improvement over the wave replication mechanism-tuned coefficients.

[26], [29]. Following these eight experiments, nine separate UAV trials successfully validated the slack tether management approach in varying head-on wave heights of 1.0 m – as well as two trials of random period irregular waves heights of 0.6 m. The trials were performed using alternating feedback methods for position: first using ground-truth motion capture feedback and then Kalman filter feedback using the de-rated ground-truth to replicate the dGPS sensor at 4 Hertz.

## B. Indoor Wave-Pool Results

1) Surrogate UAV Testing: Using the twiddle algorithm as defined in our previous work [26], standard deviation gains for the filter were tuned to  $\sigma_z = 0.0025585$ ,  $\sigma_{\dot{z}} = 1.2157e - 07$ ,  $\sigma_{\ddot{z}} = 0.77844, \ \sigma_{\mu_1} = 8.0619e - 07, \ \sigma_{\mu_2} = 2.1881e - 08,$  $\sigma_{\Delta \ddot{z}_{Acc_1}} = 326.11, \ \sigma_{\Delta \ddot{z}_{Acc_2}} = 93.507, \ \text{and when a relative}$ position measurement exists,  $\sigma_{\Delta z_{dGPS}} = 0.01$ , otherwise  $\sigma_{\Delta z_{dGPS}} = \infty$ . A typical result for one of the periodic wave profiles is shown in Figure 5. The filter properly fills in the gaps between the de-rated motion-capture (MoCap) measurements. Noticeably, the filter using the values tuned previously for the wave replication mechanism (3-PSR) performed poorly with significant overshoot at each change in direction. This was expected as the on-water experimentation has no actuator and resonance noise from the wave replication mechanism. Similar results can be seen in Figure 6, which shows the results for an irregular wave. Quantitatively, with the exception of flat water, the improvement in the filter is clearly seen in the mean error and root mean square error (RMSE) shown in Table I. The newly-tuned filter performed nearly three times better than

TABLE I ESTIMATION FILTER ERROR

	Flat Water	Periodic Waves	Irregular Waves
Test Time (s)	811.2	2044.3	129.9
$\Delta \tilde{z}   \text{Error}   \text{ (m)}$	0.0024	0.0055	0.0031
$\Delta \tilde{z}   \text{RMSE (m)}$	0.0035	0.0098	0.0049
$\Delta \tilde{z}_{PSR}$  Error  (m) $\Delta \tilde{z}_{PSR}$ RMSE (m)	0.0013	0.0187	0.0088
	0.0017	0.0252	0.0143

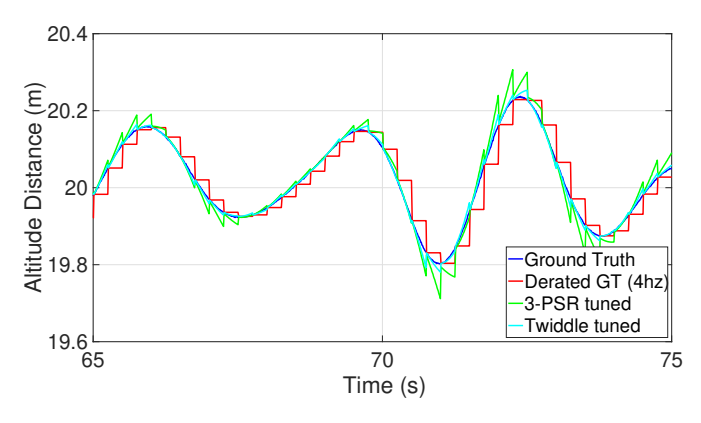


Fig. 6. Sample twiddle tuning results for a random excitation wave, showing the improvement over the wave replication mechanism-tuned coefficients

the filter tuned to the 3-PSR wave replication mechanism – minimizing the estimation error. While it would be ideal for the filter to perform equally well for flat water, this limitation is acceptable as perfectly-flat water is an extremely unlikely operating condition to exist in an actual deployment scenario.

2) UAV Flight Testing: Following the re-tuning of the estimation filter, 11 separate UAV flight testing trials successfully validated the slack-hanging tether management approach in head-on waves. Figure 7 shows a snapshot of a typical test – showing the view from the front, onboard, and profile of the experiment. The catenary model-based control performed well with the tether retaining the shape of a catenary curve throughout the wave motion profile. A typical altitude result is shown in Figure 8. The UAV has significantly more altitude variation than the USV due to the fact that the UAV was flown via remote control (RC) from shore without any position-holding controller. Noticeably, the periodicity of the wave does not show up in the UAV's motion – as would be expected in a taut tether management scenario.

To further demonstrate the decoupling of the UAV and USV motion, the normalized cross-correlation of the UAV and smart-reel altitude for a typical trial is shown in Figure 9. The amplitude of the cross-correlation is relatively flat for all time shifts – under a normalized 0.01. If the tether were pulling on the UAV, a peak near zero lag would be expected. This

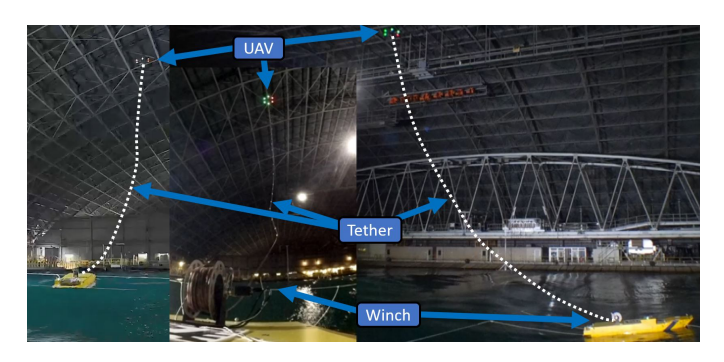


Fig. 7. MASK tethered-UAV flight testing showing a) frontal view, b) onboard view looking up at the UAV, and c) profile view. The tether is highlighted with a white dashed line for visibility.

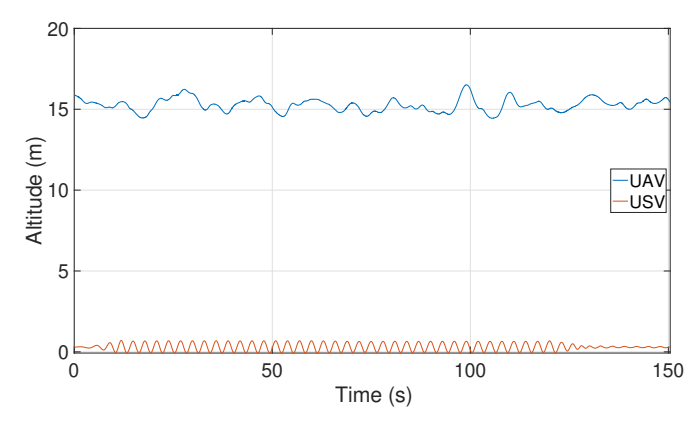


Fig. 8. UAV and smart-reel platform altitude measurements during a typical wave trial

decoupling result was typical for both pure motion capture feedback as well as Kalman filter-based feedback. One of the key takeaways of this experimentation is the three-dimensional (3-D) dynamic motion datasets of the UAV, the USV and smart-reel, and the tether nodes. A 3-D plot from a typical experiment is shown in Figure 10 and a time series plot of the altitude for all the motion tracker markers is shown in Figure 11. This dataset will serve as a valuable resource for further validating 3-D dynamic tether simulation models currently under development.

## IV. OUTDOOR SEA TRIALS

Prior to performing sea trials, an update to the reference model and significant hardware and software improvements were required.

## A. Reference Model Updates

During initial experimentation, for operating conditions with a large relative position ratio,  $\Delta r/\Delta z>3$ , using the reference model in Eq. 1 and Eq. 2 resulted in the tether having too much slack. The empirical analysis performed in our prior work [28] was repeated for a  $\Delta r/\Delta z$  up to 10 (previously only 1.2). The non-dimensionalization and curve-fit resulted in a 4th-order

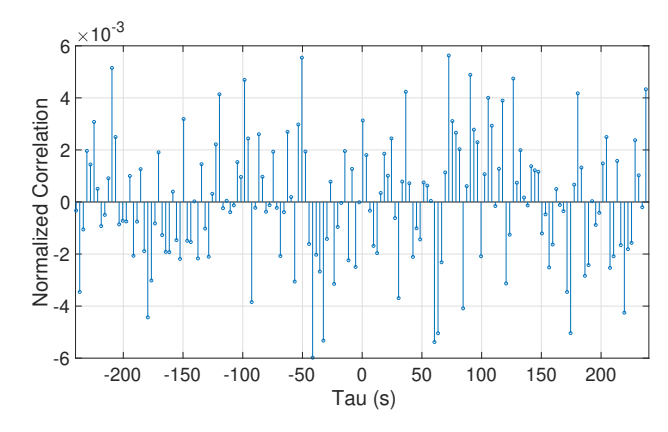


Fig. 9. Normalized cross-correlation between UAV altitude and smart-reel platform height. The low correlation demonstrates a successful decoupling of UAV flight from the USV motion.

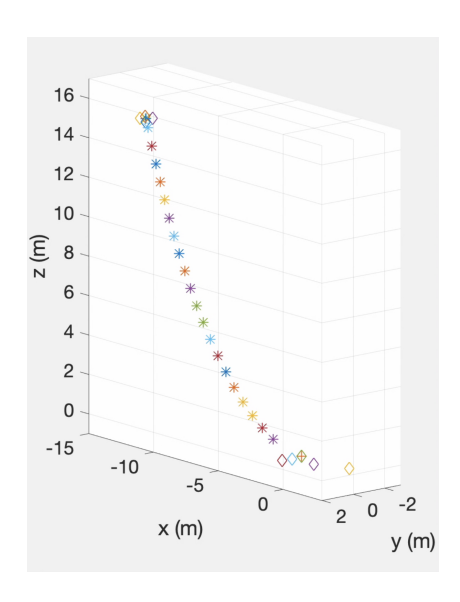


Fig. 10. This is an example of a typical 3-D motion capture dataset with the UAV defined by four points, the USV and winch defined by five points, and 20 tether markers visible.

polynomial tether reference length model which was used for all outdoor sea trials:

$$L_{ref} = \Delta z \left( f_1 + f_2 \frac{\Delta r}{\Delta z} + f_3 \frac{\Delta r^2}{\Delta z^2} + f_4 \frac{\Delta r^3}{\Delta z^3} + f_5 \frac{\Delta r^4}{\Delta z^4} \right).$$
 (5)

The curve-fit is gain-scheduled with coefficients  $f_1=0.9931$ ,  $f_2=0.1825$ ,  $f_3=0.4132$ ,  $f_4=-0.1160$ , and  $f_5=0.0134$ , and for  $\Delta r/\Delta z<2.7$ , and  $f_1=0.7023$ ,  $f_2=0.6736$ ,  $f_3=0.0784$ ,  $f_4=-0.0095$ , and  $f_5=0.0005$  for  $\Delta r/\Delta z>3.3$ . A linear combination of the two coefficient sets was used in the region of  $2.7 \le \Delta r/\Delta z \ge 3.3$ 

## B. Hardware/Software Improvements

During the indoor wave-pool MASK testing, a power surge caused damage to our microprocessor and USB hub. As a result, both the electronic hardware and software underwent modifications post-MASK-testing and prior to sea trials to improve their performance and reliability.

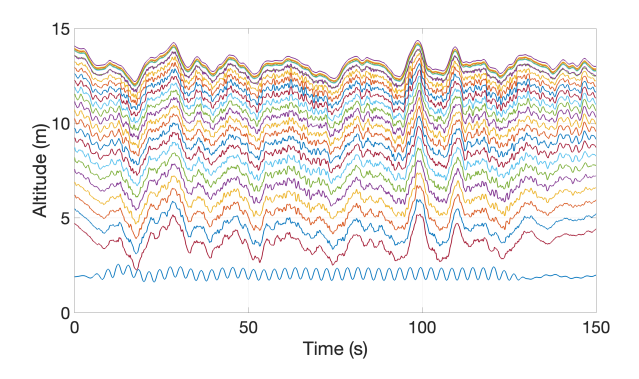


Fig. 11. Example of the motion capture dataset showing the time series altitude of the 20 tether markers, the UAV, and the smart-reel

The electronic hardware was upgraded to include industrial and marine-grade components, including a buck-boost power conditioner, in a new waterproof enclosure for added protection against harsh marine conditions. The power conditioner was designed to ensure that a constant voltage is received and voltage spikes are eliminated. In addition, the dGPS system was upgraded from the UBlox M8N chipset, which operates at 4 Hz, to the newer UBlox F9P chipset, capable of operating at 8 Hz, to improve the performance of the Kalman filter. DGPS systems are limited in their performance as dropped RTCM messages often result in a minimum of 1 second up to 5 second delays in relative position output. The dead-reckoning portion of the Kalman filter (when there are no dGPS measurements) tends to walk and affects performance after 2 seconds without a dGPS measurement update. Thus, significant effort was put into the setup of the Airborne Innovations Picoradio radios on each end of the tether (TCP/IP with 921600 Baud) to limit latency to ensure that no dGPS packets were dropped.

The software described in our previous work [26] was also modified to ensure optimal performance and timing capabilities. The CUI (Cursor User Interface) was implemented to run on a single-board, single-processor, non-real-time Beaglebone Blue computer. The Beaglebone Blue boasts an AM335x 1GHz ARM® Cortex-A8 processor and 512MB DDR3 RAM – which provide enough computing power to retrieve sensor data, run the estimation filter and controller, send command signals to actuators, record the data, display sensor status on the screen, and allow for manual control of mode states and actuators. The Beaglebone Blue also has 2×32-bit 200-MHz programmable real-time units (PRUs) that the software utilizes to meet timing needs.

To meet its timing deadlines and ensure deterministic timing, the software was modified in two ways: First, thread signals were employed to reduce the workload on the PRU by allowing background threads to convert data to binary and log it to a CSV file upon program/run termination. Second, the software was modified to convert the serial communication mechanisms from synchronous to asynchronous using Boost async\_read and async\_write functions for serial ports and sockets. These modifications allowed the PRU to receive data at a rate it governs and obtain the most up-to-date data for each sensor. Prior to these modifications, the data conversion and file-writing significantly impacted the loop rate for our controller when performed at every iteration. By ensuring that the Kalman filter, controller, and output command to the motor all occur at their desired frequencies, any buildup of errors and delays was minimized - resulting in improved performance while still providing real-time logging capabilities.

Overall, these hardware and software modifications improved the performance and reliability of the system – resulting in smoother operation of the tether management system and more accurate data. Up to an hour of data can be logged per program session without filling up the RAM – which is more than enough data for a single experimental run.

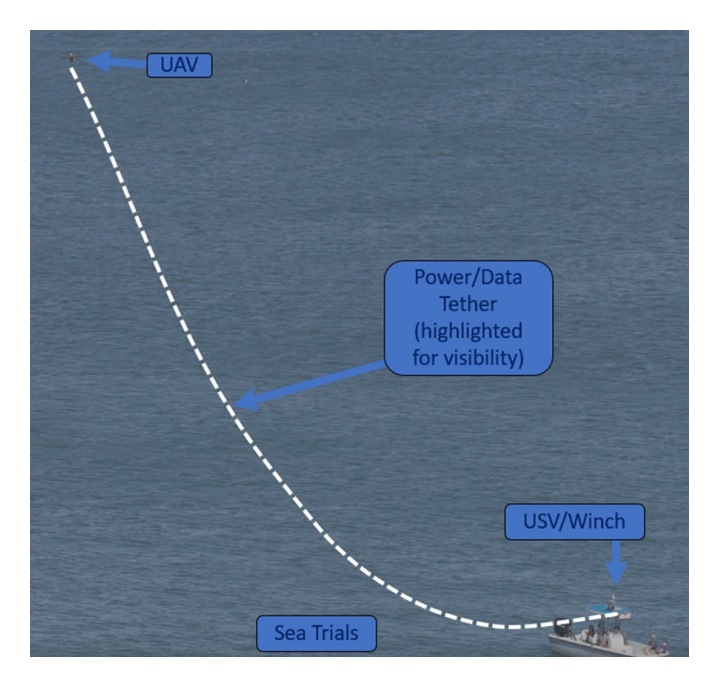


Fig. 12. Typical outdoor sea trials with the Boston Whaler at anchor in sea state 3 (up to 1.0 m waves and up to 15 knots wind). The waves varied from on-beam to aft as the boat rotated around the anchor.

## C. Sea Trial Test Setup

Three separate 30-minute flight sea trials were conducted with a Boston Whaler Guardian 22 anchored at Ballast Point, located just outside San Diego Bay, in sea state 3 (with waves up to 1.0 m and wind up to 15 knots). The waves varied from on-beam to aft as the boat rotated around the anchor. Figure 12 shows a profile view of the sea trial testing setup. The new waterproof enclosure and the smart-reel system were securely mounted onto the bimini of the 6.5 m Boston Whaler. The UAV was launched by hand from the boat, flown a short distance to the boat's beam, and then the tether management system was activated. The UAV, again RC-piloted, maintained an altitude of approximately 25 m with a relative position ratio of  $1 \leq \Delta r/\Delta z \leq 2$ .

#### D. Results

Because the outdoor sea trials had no ground-truth to compare to, the criteria for success is more qualitative than quantitative. Throughout the three sea trials, there were no missed dGPS messages – indicating that the hardware and software systems were working well. The tether was kept in a catenary shape with sufficient slack to prevent it from pulling on the UAV but not so much slack as to become fouled by the boat, anchor, or sea surface. A screenshot from an onboard camera is shown in Figure 13. The tether, with a clear catenary shape, is again highlighted for visibility. Typical tether results are shown in Figure 14. The controller performed as desired: properly switching between the purely Kalman filter-based tether reference length and the low-passed reference length. The performance of the tether management system was as desired and the experimentation was a success.



Fig. 13. This depicts an onboard view of a successful sea trial. The tether, highlighted for visibility, maintained a catenary shape throughout the 30 minute experiment.

#### V. CONCLUSION

A semi-slack, hanging tether model for tether management of a UAV-USV team underwent improvements and was experimentally validated in relevant dynamic environments including indoor wave-pool testing and sea trials. The previously developed smart-reel and its mechanical and electronic components were improved, along with the software, which was modified to implement the CUI framework and ensure deterministic operation. The semi-slack, hanging tether model, which relies on the relative position between the UAV and USV, was extended to operate through a larger relative position range up to 10.0. With the goal of outdoor operation, the estimation filter was tuned for on-water usage using experimental data from an indoor MoCap system as a groundtruth measurement. The wave-pool and sea trials confirmed the success of this approach. The development and validation of an autonomous hanging tether management system for a UAV-USV team operating in a dynamic ocean environment

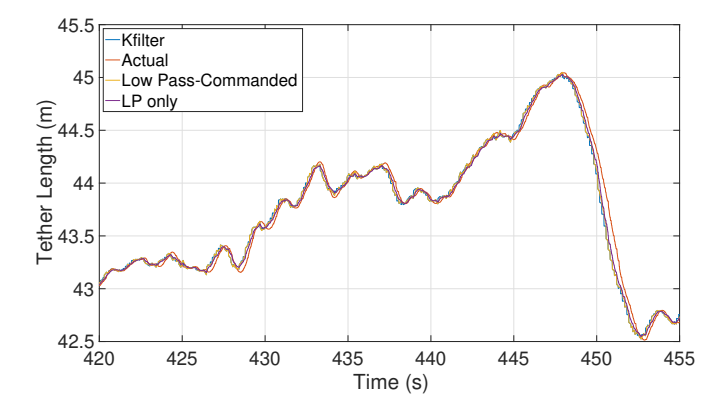


Fig. 14. This shows typical tether length results with the purely Kalman filter-based tether length, the actual tether length, the gain-scheduled low-pass commanded tether length, and a purely low-pass hypothetical tether length.

up to sea state 4 is a significant technical achievement with far-reaching implications. The system's ability to manage a slack, hanging tether has been validated through both wave-pool testing and on-water sea trials, demonstrating robustness to heave and pitch motions of the USV. In effect, increasing the UAV's payload capacity and altitude limits. Until the present work, the comprehensive demonstration and documentation of this critical capability has not been thoroughly demonstrated. Additionally, the generation of a unique UAV-tether-USV dynamic motion dataset provides a valuable resource for validating tether dynamic simulation models.

The ability to successfully fly a tethered UAV from a highly dynamic USV has important implications beyond military applications. For example, the fishing industry can benefit from the ability to conduct more efficient and cost-effective surveys of fish populations. Environmental conservation efforts can also benefit from the system's ability to collect high-quality data over a larger area than previously possible – improving the understanding of the ocean's ecosystems. This system also has potential applications in oceanographic research where it can be used to monitor oceanographic phenomena such as ocean currents and eddies – improving our understanding of the Earth's climate system. This work represents a significant step forward in the application of autonomous, longendurance, tethered UAVs.

## REFERENCES

- J. Kim, B. D. Song, and J. R. Morrison, "On the scheduling of systems of UAVs and fuel service stations for long-term mission fulfillment," *Journal of Intelligent & Robotic Systems*, vol. 70, pp. 347–359, Apr 2013
- [2] S. Y. Choi, B. H. Choi, S. Y. Jeong, B. W. Gu, S. J. Yoo, and C. T. Rim, "Tethered aerial robots using contactless power systems for extended mission time and range," in 2014 IEEE Energy Conversion Congress and Exposition (ECCE), pp. 912–916, Sept 2014.
- [3] C. Papachristos and A. Tzes, "The power-tethered UAV-UGV team: A collaborative strategy for navigation in partially-mapped environments," in 22nd Mediterranean Conference on Control and Automation, pp. 1153–1158, June 2014.
- [4] L. Sandino, M. Bejar, K. Kondak, and A. Ollero, "Advances in modeling and control of tethered unmanned helicopters to enhance hovering performance," *Journal of Intelligent & Robotic Systems*, vol. 73, no. 1, pp. 3–18, 2014.
- [5] G. Schmidt and R. Swik, "Automatic hover control of an unmanned tethered rotorplatform," *Automatica*, vol. 10, pp. 393–394, Jan. 1974.
- [6] D. Ferreira de Castro, J. S. Santos, M. Batista, D. Antônio dos Santos, and L. C. Góes, "Modeling and control of tethered unmanned multicopters in hovering flight," in AIAA Modeling and Simulation Technologies Conference, American Institute of Aeronautics and Astronautics, June 2015.
- [7] S. Lupashin and R. D'Andrea, "Stabilization of a flying vehicle on a taut tether using inertial sensing," in 2013 IEEE/RSJ International Conference on Intelligent Robots and Systems, pp. 2432–2438, Nov 2013.
- [8] M. M. Nicotra, R. Naldi, and E. Garone, "Taut cable control of a tethered UAV," *IFAC Proceedings Volumes*, vol. 47, no. 3, pp. 3190 – 3195, 2014. 19th IFAC World Congress.
- [9] Y. Ouchi, K. Kinoshita, K. Watanabe, and I. Nagai, "Control of position and attitude of the tethered X4-Flyer," in 2014 IEEE/SICE International Symposium on System Integration, pp. 706–711, Dec 2014.
- [10] L. A. Sandino, M. Bejar, K. Kondak, and A. Ollero, "On the use of tethered configurations for augmenting hovering stability in smallsize autonomous helicopters," *Journal of Intelligent & Robotic Systems*, vol. 70, no. 1, pp. 509–525, 2013.

- [11] B. Ahmed and H. R. Pota, "Backstepping-based landing control of a RUAV using tether incorporating flapping correction dynamics," in 2008 American Control Conference, pp. 2728–2733, June 2008.
- [12] S.-R. Oh, K. Pathak, S. K. Agrawal, H. R. Pota, and M. Garratt, "Approaches for a tether-guided landing of an autonomous helicopter," *IEEE Transactions on Robotics*, vol. 22, pp. 536–544, June 2006.
- [13] L. A. Sandino, D. Santamaria, M. Bejar, A. Viguria, K. Kondak, and A. Ollero, "Tether-guided landing of unmanned helicopters without GPS sensors," in 2014 IEEE International Conference on Robotics and Automation (ICRA), pp. 3096–3101, May 2014.
- [14] M. M. Nicotra, R. Naldi, and E. Garone, "Nonlinear control of a tethered UAV: the taut cable case," CoRR, 2016.
- [15] F. M. Briggs IV and T. Stave, "Reactive tether spool," Sept. 14 2017. US Patent App. 15/456,096.
- [16] M. Tognon, S. S. Dash, and A. Franchi, "Observer-based control of position and tension for an aerial robot tethered to a moving platform," *IEEE Robotics and Automation Letters*, vol. 1, pp. 732–737, July 2016.
- [17] A. Kourani and N. Daher, "Bidirectional manipulation of a buoy with a tethered quadrotor uav," in 2021 IEEE 3rd International Multidisciplinary Conference on Engineering Technology (IMCET), pp. 101–106, 2021.
- [18] A. Kourani and N. Daher, "Marine locomotion: A tethered uav-buoy system with surge velocity control," *Robotics and Autonomous Systems*, vol. 145, p. 103858, 2021.
- [19] A. Kourani and N. Daher, "Three-dimensional modeling of a tethered uav-buoy system with relative-positioning and directional surge velocity control," *Nonlinear Dynamics*, vol. 111, pp. 1245–1268, Jan 2023.
- [20] L. Zikou, C. Papachristos, and A. Tzes, "The power-over-tether system for powering small UAVs: Tethering-line tension control synthesis," in 2015 23rd Mediterranean Conference on Control and Automation (MED), pp. 681–687, June 2015.
- [21] L. A. Sandino, M. Bejar, K. Kondak, and A. Ollero, "A square-root unscented Kalman filter for attitude and relative position estimation of a tethered unmanned helicopter," in 2015 International Conference on Unmanned Aircraft Systems (ICUAS), pp. 567–576, June 2015.
- [22] A. Al-Radaideh and L. Sun, "Self-localization of a tethered quadcopter using inertial sensors in a GPS-denied environment," in 2017 International Conference on Unmanned Aircraft Systems (ICUAS), pp. 271–277, June 2017.
- [23] B. Galea and P. G. Kry, "Tethered flight control of a small quadrotor robot for stippling," in 2017 IEEE/RSJ International Conference on Intelligent Robots and Systems (IROS), pp. 1713–1718, Sept 2017.
- [24] S. Kiribayashi, K. Yakushigawa, and K. Nagatani, "Position estimation of tethered micro unmanned aerial vehicle by observing the slack tether," in 2017 IEEE International Symposium on Safety, Security and Rescue Robotics (SSRR), pp. 159–165, Oct 2017.
- [25] A. Borgese, D. C. Guastella, G. Sutera, and G. Muscato, "Tether-based localization for cooperative ground and aerial vehicles," *IEEE Robotics* and Automation Letters, vol. 7, no. 3, pp. 8162–8169, 2022.
- [26] K. Talke, F. Birchmore, and T. Bewley, "Autonomous hanging tether management and experimentation for an unmanned air-surface vehicle team," *Journal of Field Robotics*, vol. 39, no. 6, pp. 869–887, 2022.
- [27] K. Talke, D. Drotman, N. Stroumtsos, M. Oliveira, and T. Bewley, "Design and parameter optimization of a 3-PSR parallel mechanism for replicating wave and boat motion," in 2019 IEEE International Conference on Robotics and Automation (ICRA), May 2019.
- [28] K. Talke, M. Oliveira, and T. Bewley, "Tether shape analysis for a UAV USV team," in 2018 IEEE International Conference on Intelligent Robots (IROS), Oct 2018.
- [29] S. Thrun, W. Burgard, and D. Fox, Probabilistic robotics. MIT press, 2005.